

Evaluation of AVHRR cloud detection at Dome Fuji Station, Antarctica

Takashi Yamanouchi¹, Naohiko Hirasawa¹, Gaku Kadosaki^{2*} and Masahiko Hayashi³

¹National Institute of Polar Research, Kaga 1-chome, Itabashi-ku, Tokyo 173-8515

²Faculty of Science, Kochi University, Kochi 780-8520

³Fukuoka University, Nanakuma, Jonan-ku, Fukuoka 814-0180

Abstract: A polar cloud detection algorithm, which uses the scatter diagram of brightness temperature and brightness temperature difference of $10\ \mu\text{m}$ split window channels of AVHRR, was evaluated at Dome Fuji Station, Antarctica. Among the data of June 1997, most of the cloudy scenes were effectively detectable. However, some of the cloudy scenes were not detectable with only the scatter diagram. It was found that additional information on the temporal variation of brightness temperature permitted effective detection.

1. Introduction

Polar cloud climatology from satellite data is still not well understood (Rossow and Shiffer, 1999; Stubenrauch *et al.*, 1999). In the polar regions over snow covered surfaces, a simple cloud detection algorithm for visible or infrared data will be confronted with difficulties due to high albedo and low temperature of snow surface, which makes the contrast between cloud and snow surface small. Extensive efforts have been devoted to the analysis of polar cloud detection from satellite passive measurements (*e.g.*, Raschke, 1987; Lubin *et al.*, 1998; Muramoto *et al.*, 1998); however, the cloud detection algorithm still has problems during the long polar night when only the infrared channels can be used.

In the present paper, cloud detection using brightness temperature and brightness temperature difference in $10\ \mu\text{m}$ split window channels of AVHRR (Advanced Very High Resolution Radiometer; Yamanouchi *et al.*, 1987; Yamanouchi and Kawaguchi, 1992) was validated from surface observations in winter at Dome Fuji Station ($77^{\circ}19'S$, $39^{\circ}42'E$, 3800 m a. s. l.; Fig. 1), inland Antarctica. We had a valuable opportunity for wintering observation for atmospheric science by 38th Japanese Antarctic Research Expedition (JARE-38) under the project "Atmospheric Circulation and Material Cycle in the Antarctic" at Dome Fuji Station in 1997 (Yamanouchi *et al.*, 1999), following two years of wintering for deep ice core drilling (Fujii *et al.*, 1999).

2. Data

AVHRR data were derived from the NOAA HRPT (High Resolution Picture

* Present address: Department of Polar Science, The Graduate University for Advanced Studies, Kaga 1-chome, Itabashi-ku, Tokyo 173-8515.

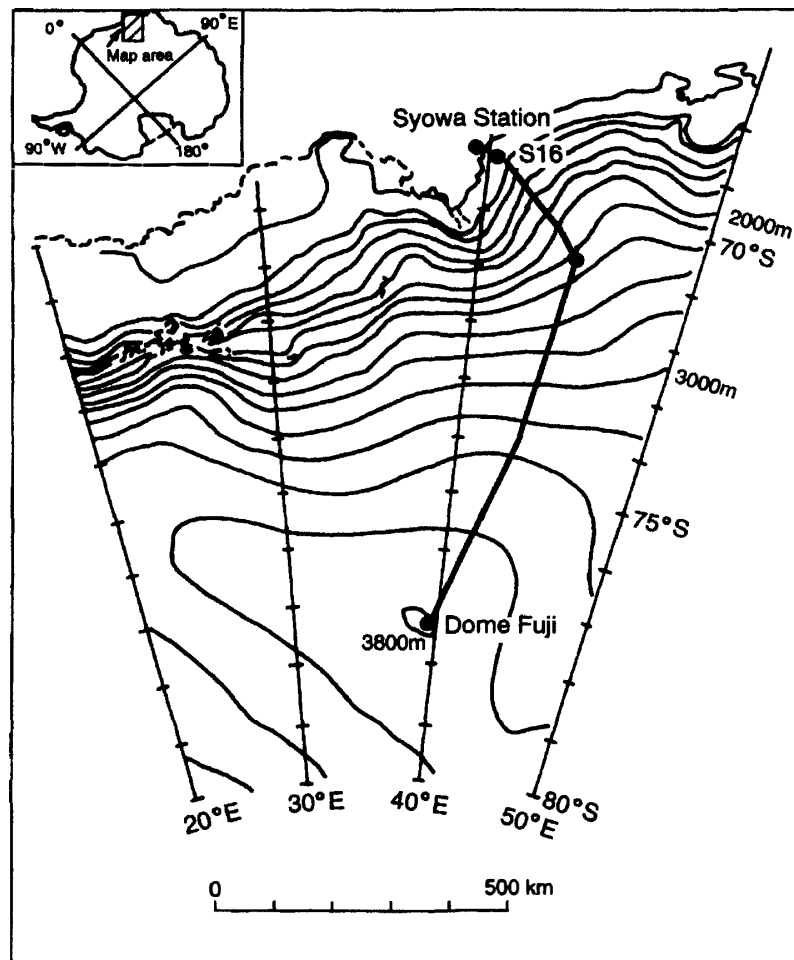


Fig. 1. Location of Dome Fuji Station in inland Antarctica. The thick line indicates the traverse route from Syowa Station.

Transmission) data directly received at Syowa Station using a newly installed receiving-archiving system (Sea Space Inc.). 128×128 pixels with 2.2 km resolution are sampled from about a 300 km square around Dome Fuji Station and 4×4 pixels are averaged as each data point. Then 32×32 data points are used.

The satellite data are compared with data from synoptic observations including cloud amount, aerological soundings, surface radiation measurements and lidar measurements at Dome Fuji Station by JARE-38 in 1997.

3. Results and discussion

As shown in Fig. 3 from Yamanouchi and Kawaguchi (1992) as a successful example, we tried to make a scatter plot of data for the pixel covering Dome Fuji Station. Figure 2 shows the scatter plot of brightness temperature difference of channels 3 and 4 ($T_3 - T_4$) against brightness temperature of channel 4 (T_4). Though the AVHRR channel 3 data in the $3.7 \mu\text{m}$ spectral region, in principle, provide information on clouds even without solar reflection, they contain large variability up to 40°C at low

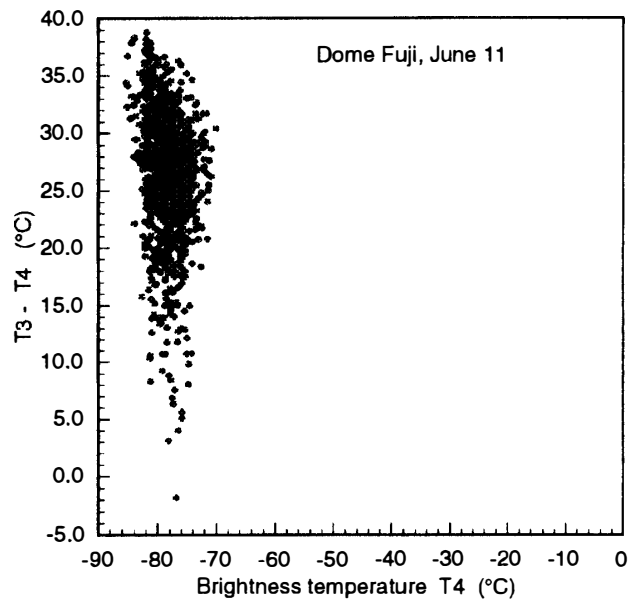


Fig. 2 Scatter diagram of $T_3 - T_4$ against T_4 at Dome Fuji Station on June 11, 1997.

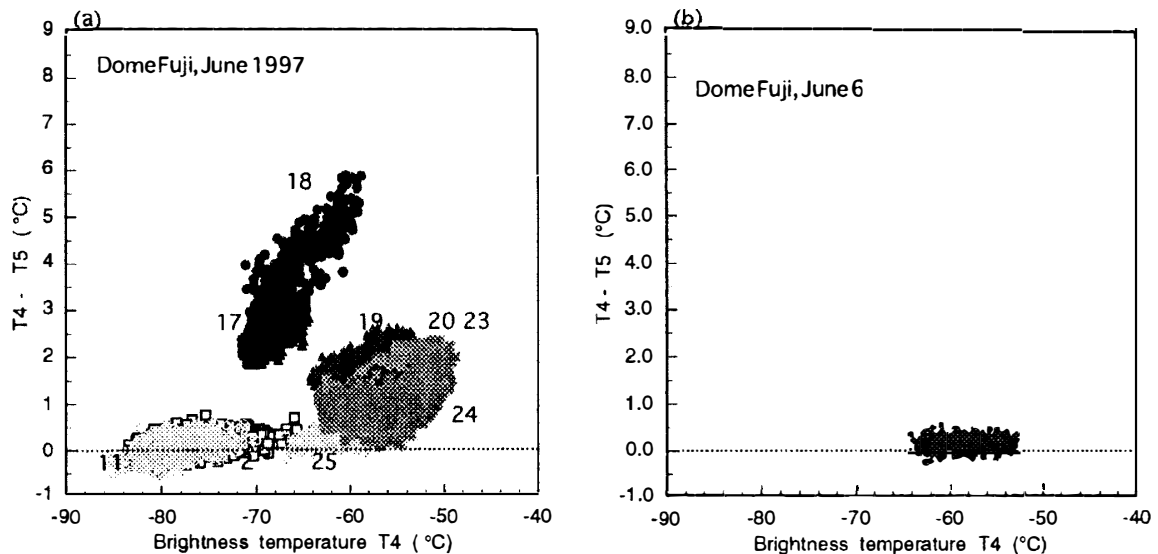


Fig. 3. (a) Scatter diagram of $T_4 - T_5$ against T_4 for clear days (June 2, 11, 25) and for overcast days (June 17, 18, 19, 20, 23 and 24), respectively, in June 1997 at Dome Fuji Station. (b) Scatter diagram of $T_4 - T_5$ against T_4 for low-level cloud on June 6, 1997 at Dome Fuji Station.

temperatures such as -80 and -90°C due to low temperature resolution, and are difficult to use.

Figure 3 shows the scatter plot of brightness temperature difference of channels 4 and 5 ($T_4 - T_5$) against brightness temperature of channel 4 (T_4). Typical results from 9 days (9 passes) in June 1997 are shown in Fig. 3a; data on June 2, 11 and 25, when the surface observer reported clear sky; data on June 17 and 18, when the surface reports

were overcast with blizzard; and data on June 19, 20, 23 and 24, when the sky was covered with cloud amount larger than 8. In case of clear sky, data points were distributed around the line $T_4 - T_5 = 0$, with the range of T_4 between -85 to -60°C . On June 17 and 18, T_4 ranged between -72 and -58°C , and $T_4 - T_5$ was distributed widely between 2 and 6°C , easily detectable as cloudy. On other cloudy days, June 19 to 24, $T_4 - T_5$ still showed some distinction from 0°C and these pixels were detectable as cloudy. The large brightness temperature difference must be due to the smaller optical thickness of the cloud layer observed from the satellite (Yamanouchi *et al.*, 1987; Yamanouchi and Kawaguchi, 1992), for example as cirrus (Ci) (Inoue, 1987). These data all show a possibility of cloud detection using $T_4 - T_5$.

On the other hand, Fig. 3b shows the similar scatter plots for July 6, when the surface reports indicated cloud amount 8 with cirrostratus (Cs). Examining the results of longwave radiation measurements as shown in Fig. 4a, increased downward radiation assured the cloudy condition on this day. From Fig. 3b, data points lie along the line $T_4 - T_5 = 0$, and are difficult to distinguish from clear cases as seen in Fig. 3a. However, the range of T_4 is very high, about -65 to -50°C , which might be an indication of a cloudy condition.

Figure 4b shows the average T_4 , average $(T_4 - T_5)$ and cloud amount reported by surface observers at the time of the satellite pass. As mentioned above, most of cloudy skies make $T_4 - T_5$ large, and can be discriminated from clear skies. However, in some cases, such as 6 and 13 June, $T_4 - T_5$ was nearly 0, indistinguishable from the clear case. However, in these cases, T_4 itself shows an abrupt increase from the day before, and from the variation of T_4 , it is possible to say that it was cloudy. In these cases, it is expected that clouds will be low-level, stratiform and have large optical thickness, and lie in the high temperature layer just above the surface inversion. Once clouds cover the area, downward radiation increases along with the surface temperature and upward radiation (Fig. 4a). The problem is that large T_4 does not always imply that it is cloudy. If a warm air mass intrudes into the inland area, the surface temperature also will increase. So, theoretically, it is not possible to determine that it is cloudy only from the high brightness temperature. The clear sky on June 25, showing a higher T_4 in Fig. 3a, is such a case; June 25 is among a few days when higher temperature continued. Actually, only the abrupt increase of T_4 on a daily scale is acceptable that it is cloudy. Consequently, most cases of cloudy skies, at least all cases with cloud amount larger than 5 in June 1997, were detected with T_4 and $T_4 - T_5$ of AVHRR.

Atmospheric vertical profiles can be discussed from lidar and aerological data. From lidar measurements (Hayashi, 1999), vertical profiles of clouds were roughly seen and continuous cloud from near the surface to 5 km height (from ground surface) was confirmed for June 6, while layered cloud was observed to be distributed intermittently from 2 to 9 km height on June 23. From aerological soundings made at the station (Hirasawa *et al.*, 1999), 41 temperature profiles were obtained during June. All the profiles show a strong surface inversion. Except during 17 to 21, in a blocking condition to be explained later, the strength of the surface temperature inversion was between 15 and 20 degrees on 6, 13, 14, 15 and 25, when higher cloud amount existed, and more than 20 degrees on other days. Referring to the cloud top height obtained from lidar data, on June 6, the cloud top temperature was about -62°C and the

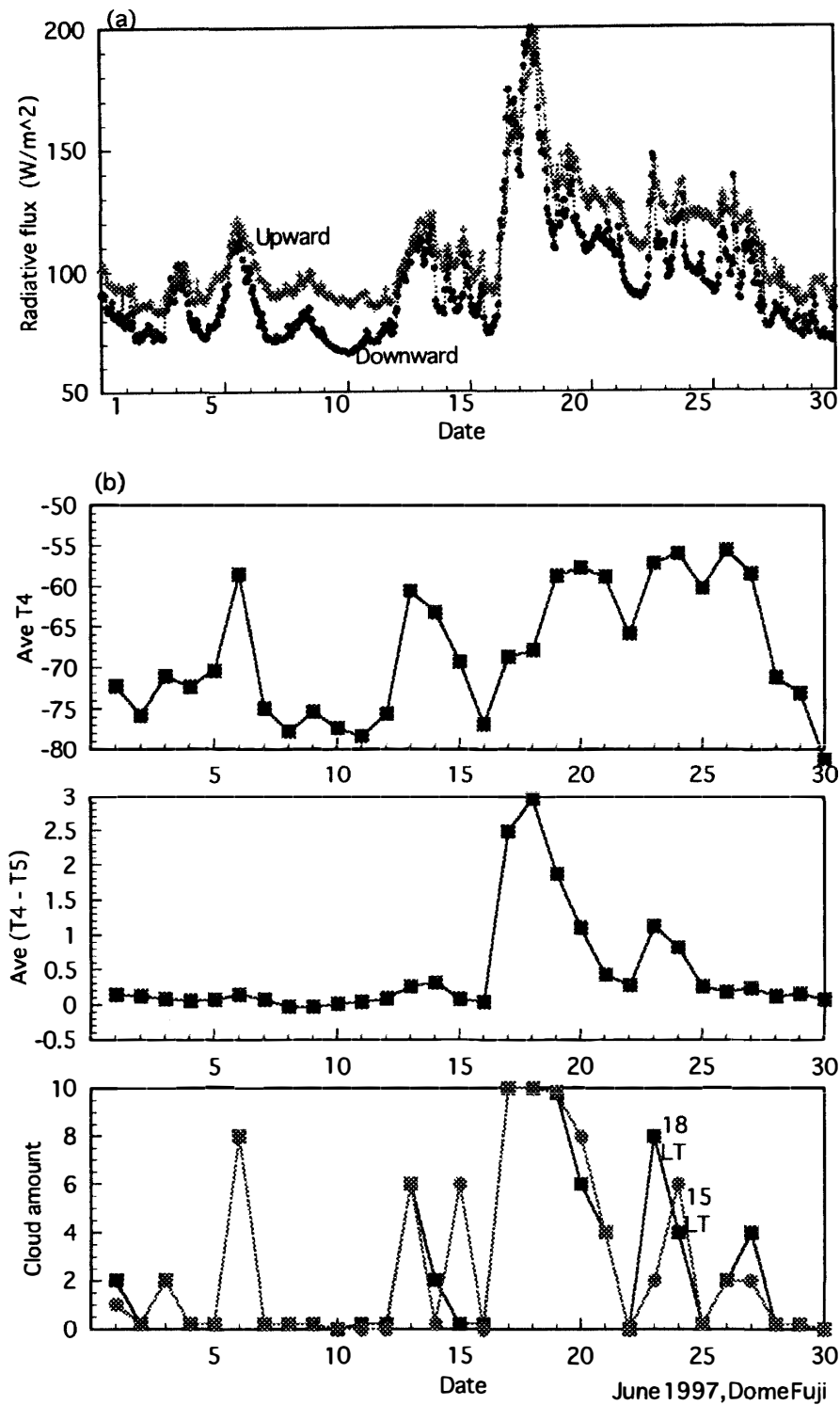


Fig. 4. (a) Hourly longwave radiative fluxes measured at the surface of Dome Fuji Station. (b) Average T_4 , average $(T_4 - T_5)$ from AVHRR around Dome Fuji Station and cloud amount reported by surface observers at the time of the satellite pass.

difference from the surface temperature was only about 5 degrees, which must have resulted in the small brightness temperature difference regardless of cloud optical thickness. On the other hand, on June 23, the cloud top temperature was about -75°C , more than 25 degrees below the surface temperature.

Let us return to the variation of longwave radiation flux shown in Fig. 4a. The base line for the downward longwave flux is about 70 to 80 W/m^2 , which is for a clear day. Increase of about 30 to 50 W/m^2 is frequently seen due to the covering by clouds. However, sometimes, such as on 17 to 18 June, there is a tremendous increase of downward flux, of up to 200 W/m^2 . Upward flux also follows a similar increase. This great increase can be caused not only by the cloud radiative effect, but also by warm and moist air intruding onto the high plateau under the "blocking condition". This phenomena has already been explained in detail by Hirasawa *et al.* (2000). Once the blocking high is settled, warm and moist air can advect onto the high plateau of inland Antarctica, and surface air temperature increases greatly. In the present case, the increase of the surface temperature was, surprisingly, more than 40°C . From aerological observations, the temperature and humidity profile changed greatly throughout the troposphere, and absolutely different air mass, such as of mid-latitude intruded into the Antarctic. This great change in the air mass resulted in a great change of the radiation. The role of these phenomena in the energy transfer in the polar regions is a matter for future discussion.

4. Concluding remarks

Using the scatter plot of brightness temperature difference $T_4 - T_5$ against brightness temperature T_4 , most of the cloudy scene was detectable with large brightness temperature difference. Using the temporal variation, some scenes which had small brightness temperature difference still could be detected as cloudy, when T_4 increased abruptly. Consequently, most cases of cloudy skies, at least all cases with cloud amount larger than 5 in June 1997, were detected with the T_4 and $T_4 - T_5$ of AVHRR.

References

- Fujii, Y. and 25 others (1999): Deep ice coring at Dome Fuji Station, Antarctica. *Nankyoku Shiryô (Antarct. Rec.)*, **43**, 162–210.
- Hayashi, M. (1999): On observation of aerosol and atmospheric minor constituents at Dome Fuji Station. *Tenki*, **46**, 153–156 (in Japanese).
- Hirasawa, N., Hayashi, M., Kaneto, S. and Yamanouchi, T. (1999): Aerological sounding data at Dome Fuji Station in 1997. Data of Project on Atmospheric Circulation and Material Cycle in the Antarctic, Part 1. *JARE Data Rep.*, **238** (Meteorology 32), 183.
- Hirasawa, N., Nakamura, H. and Yamanouchi, T. (2000): A blocking formation and the abrupt change of meteorological data at Dome Fuji Station, Antarctica. *Geophys. Res. Lett.*, **27**, 1911–1914.
- Inoue, T. (1987): A cloud type classification with NOAA 7 split-window measurements. *J. Geophys. Res.*, **92**, 3991–4000.
- Lubin, D. and Morrow, E. (1998): Evaluation of an AVHRR cloud detection and classification method over the central Arctic ocean. *J. Appl. Meteorol.*, **37**, 166–183.
- Muramoto, K., Kubo, M., Saito, H. and Yamanouchi, T. (1998): Classification of polar satellite data using minimum distance method. *Mem. Natl Inst. Polar Res., Spec. Issue*, **52**, 149–157.

- Raschke, E. (1987): Rep. International Satellite Cloud Climatology Project (ISCCP) Workshop on Cloud Algorithms in the Polar Regions. WMO/TD-170, 77 p.
- Rossow, W.B. and Schiffer, R.A. (1999): Advances in understanding clouds from ISCCP. Bull. Am. Meteorol. Soc., **80**, 2261-2287.
- Stubenrauch, C. J., Rossow, W.B., Cheruy, F., Chedin, A. and Scott, N A. (1999): Clouds as seen by satellite sounders (3I) and imagers (ISCCP). Part I: Evaluation of cloud parameters. J. Climate, **12**, 2189-2213.
- Yamanouchi, T. and Kawaguchi, S. (1992): Cloud distribution in the Antarctic from AVHRR and radiation measurements at the ground. Int. J. Remote Sensing, **13**, 111-127.
- Yamanouchi, T., Suzuki, K. and Kawaguchi, S. (1987). Detection of clouds in Antarctica from infrared multispectral data of AVHRR. J. Meteorol. Soc. Jpn., **65**, 949-962.
- Yamanouchi, T., Hirasawa, N. and Hayashi, M. (1999): Report of observation project on "Atmospheric Circulation and Material Cycle in the Antarctic" by JARE-38. Polar Meteorol. Glaciol., **13**, 159-164.

(Received March 13, 2000; Revised manuscript accepted June 23, 2000)